GAMMA SPECTROMETRIC ANALYSIS OF LOWER DANUBE SAMPLES FROM ROMANIA

by

Iulian POJAR VINTILA [1], ***Sorin UJENIUC*** [2], ***Irina CATIANIS*** [1], ***Bogdan ALEXANDRESCU*** [1], ***Albert M. SCRIECIU*** [1], ***Silvana VASILCA*** [2], ***and Rares SUVAILA*** [1,2*]

[1] National Institute for Research and Development on
Marine Geology and Geo-ecology – GeoEcoMar, Bucharest, Romania
[2] Horia Hulubei National Institute for Physics and Nuclear Engineering, Magurele, Romania

Scientific paper
https://doi.org/10.2298/NTRP2403226P

This paper focuses on the natural and anthropogenic radioactivity of sediment samples from key spots located in the Lower Danube area and the Danube Delta region. The idea of the study is to confirm that gamma spectrometry is an efficient method for geological sample characterization in terms of isotopic ratios and also for evaluating the impact of nuclear activities, namely testing artificial contamination. This is a preliminary study meant to analyze the relevance of a database for reference sediments from the Danube River built via gamma ray spectrometry.

Key words: geological sample, isotopic abundance, ecology, gamma spectrum

INTRODUCTION

Environmental sample analysis is crucial for a better understanding of our surroundings and their evolution. Particularly, radioactivity measurements provide precious information in the field of elemental analysis and also from the perspective of human exposure to ionizing radiation and the related health risks. The main component of the radioactive background originates from natural sources, from cosmic to telluric, but since the very beginning of nuclear physics, scientific, energetic and unfortunately, also non-civil activities add an anthropogenic component to the spectrum. One must distinguish between those two contributions to the overall exposure in order to correctly evaluate the implications on radioisotopic abundance, environmental influence, from simple individual constituents of the biota to consequences in the trophic chain. Recent studies confirm those topics are of great interest, as shown by Deniz and Calik in [1], from the perspective of annual effective dose equivalents and cancer risks, or by Janković *et al*. [2], who point out the importance of the tritium levels, as the latter is produced both naturally and artificially, and the second way must be rigorously monitored, for its levels are of great public concern. Gamma-ray analysis is the most spreaded method for such radiological charactetizations, as it does not require special sample preparation, but provides valuable and precise data in return.

The aim of this paper is to prove feasibility of a database for sediment characterization by non-destructive methods, particularly gamma-ray spectrometry, for the Danube region. The results are related to isotopic footprints, retrospective dosimetry, geochronological dating and artificial contamination testing. In the geological context, the present study and related continuation would help understanding sediment transport in the future and also retroactive comprehension of emergent pollutant [3] concentrations by means of time markers, radioactive decay indicators with half-lives ranging from tens to billions of years.

The scope is to start a national reference database starting at the Lower Danube, and further, with the Danube Delta, where the river splits into branches and channels, downstream to the Black Sea. Supplementary areas of interest are located along the Romanian-Bulgarian border upstream to the Serbian zone, finally tracking the isotopes towards the source of the Danube River in Germany. The plan is to achieve this with regular sized HPGe detectors (the order of 2.5 by 2 inches crystal) with average efficiency (50 % at 1332 keV) within a reasonable acquisition time (24 hours per sample for good statistics). Of course, the trade-off between acquisition time and statistical uncertainty is given by detection efficiency, background level (shielding thickness, nitrogen purge, *etc*.) and the acquisition time. A preliminary investi-

* Corresponding author, e-mail: rares.suvaila@geoecomar.ro

gation was performed here in order to confirm that the parameters explicated in the precedent paragraph are a reasonable option.

The goal is to see if the differences observed between the samples are significative such as: samples from a certain area can be considered characteristic, even if the mean values are close to those of another area nearby and samples from a relatively small area still exhibit differences that would allow tracking value evolution in time.

MATERIALS AND METHODS

Study area and sample collection

The samples were drawn from three Lower Danube and Delta areas, close to the Black Sea, which are critical for advancing the study upstream the river and characterizing the Danube sediment deposition influence on the areas nearby the spill region. A batch of 19 samples drawn at the water-sediment interface from the locations indicated in tab. 1 and fig. 1 of about 200 g (wet) were analyzed for checking if they meet the criteria for pattern recognition. The sampling equipment used was a Van Veen grab sampler.

There were two main sampling areas according to fig. 1: Sfantu Gheorghe Branch and channel system, nearby Dunavatu village (1), and the Danube splitting area (in the three main branches), north of Tulcea city (2). Additionally, two samples (positions 1 and 8) were taken from the Chilia Branch. The main components, supposed layer age and physical characteristics are significantly different, which is essential for the study, as the intention is to test and demonstrate a unified protocol for the entire study area.

Table 1. Coordinates of the sample drawing locations

No	Code	Latitude	Longitude	Depth [m]
1	DD-19-01	45°24'38.8"	29°32'04.8"	9.3
2	DD-19-08	45°18'18.4"	28°57'09.3"	17.1
3	DD-19-11	45°14'36.5"	28°47'43.5"	18.1
4	DD-19-16	45°14'03.0"	28°5'44.8"	14.2
5	DD-19-17	45°13'21.7"	28°43'10.5"	20.2
6	DD-19-20	45°13'22.7"	28°44'35.2"	20.5
7	DD-19-23	45°11'32.5"	28°48'40.5"	14.0
8	DD-19-26	45°11'50.1"	28°52'02.5"	13.5
9	DD-19-29	45°11'12.6"	28°53'50.7"	20.9
10	DD-19-32	45°10'57.0"	28°53'35.8"	13.4
11	DD-19-33	45°59'45.6"	29°17'59.9"	13.0
12	DD-19-36	45°01'13.3"	29°18'38.5"	3.4
13	DD-19-38	45°00'19.4"	29°17'05.1"	20.8
14	DD-19-41	45°01'08.9"	29°16'30.5"	19.7
15	DD-19-44	45°00'43.6"	29°16'13.0"	5.0
16	DD-19-45	45°01'30.4"	29°16'09.7"	8.3
17	DD-19-48	45°02'03.6"	29°15'46.5"	8.1
18	DD-19-49	45°02'15.5"	29°16'15.4"	9.3
19	DD-19-117	45°14'29.6"	28°54'28.5"	1.4
20	DD-BLANK	n/a	n/a	n/a

Sample preparation and calibrations

Sample preparation has been achieved in accordance with the general International Atomic Energy Agency (IAEA) [4] recommendations. The samples were dried, subsequently crushed and milled till the grain size was was below 100 m, before being sealed in sarpagan boxes of 120 cm^3 volume in order to be measured in a cylindrical geometry, on top of a HPGe detector, with a 50 mm lead shield around and 50 mm distance from any side of the detector to the shield. The detector used was a p-type Hyper Pure Germanium of 50 % relative efficiency at 1332 keV. Geometric data such as the distance between the end cap and the HPGe crystal were corrected by simulating detector-source geometries with Monte Carlo (MC) code GESPECOR [5]. The MC computations for geometric data were also needed, as the sample containers were not identical to the calibration sources, so the efficiency transfer procedure in GESPECOR [6] was applied. Standard ORTEC digital spectrum analyzer and software were used. A 50 mm thick lead shield was used for lowering the background. The calibration was performed with standard volume sources of ^{152}Eu and ^{137}Cs. Energy and peak width calibration were carried out in the standard way with ORTEC Maestro32 software.

For calibration purposes, a ^{137}Cs calibration source of (1301 ±65) Bq on Apr 1st, 2010 and a ^{152}Eu source of (689.4 ±34) Bq on Jan 1st, 1995 were used. Sample containers were all 70 mm in diameter, 37 mm high and all plastic walls were 1.5 mm thick, resulting in a 120 cm^3 interior volume. Sample masses and densities ranged between 100 g and 160 g, 0.9 gcm^{-3} and 1.3 gcm^{-3} , respectively. The HPGe dead layer was initially about 0.6 mm; after 10 years this value almost doubled; also rounded crystal corners and orientation may vary with respect to the manufacturer data. A radioscopy is shown in fig. 2. Every detail was included in the simulations. The samples were placed vertically, in a cylindrical symmetric set-up, on the top surface of the detector; the detector vicinity was purged with evaporated nitrogen from the Dewar vessel in order to lower ambiental Rn descendants' contribution to the spectra.

The extension of the calibrated energy range was done by using reference materials (RM) provided by the IAEA (such as IAEA-375 Soil) by means of yield ratios for RM radioisotopes which provided peaks in the calibrated but also in the non-calibrated parts of the spectra. Applying this method allows extending the efficiency calibration outside the source's energy interval, of course, if for each ratio one RM peak involved is actually in the calibrated area, so the efficiency for that peak can be interpolated prior to extrapolating related peaks outside the interval [7]. Additional MC simulations have been performed in order to apply the correction factors using the GESPECOR code. The source-detector geometry was identical for all the samples, but there is a need to have auto-attenuation corrections and coincidence summing ones, although

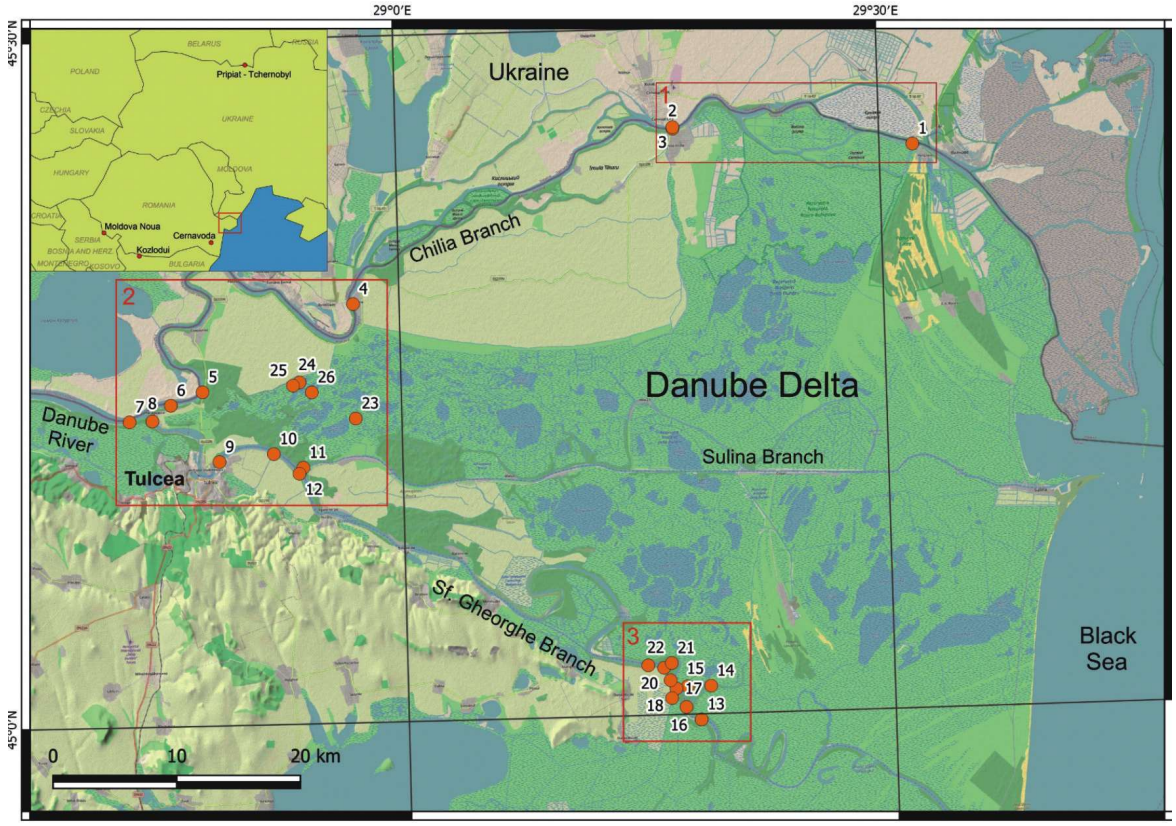

Figure 1. Map of the sampling locations*

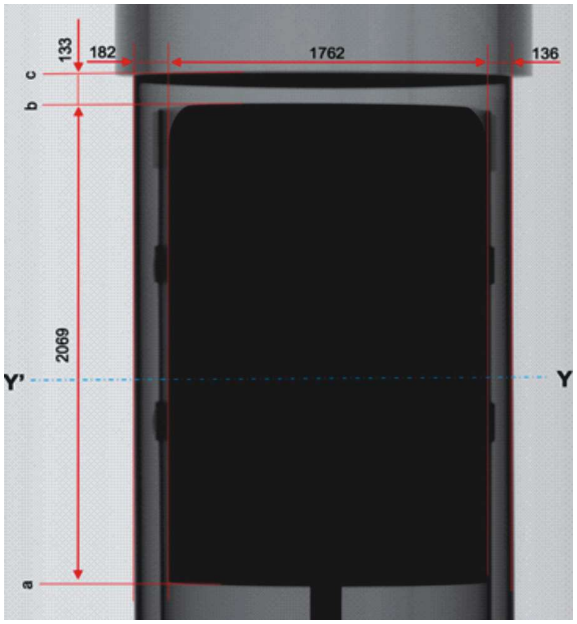

Figure 2. Radioscopy of an ORTEC HPGe detector showing precise dimensions **

the latter were all below 1 % for this batch, since everything contributes to the uncertainty budget, as explicated in the next paragraph. Sample uniformity was carefully ensured, which is considered an important issue, as pointed out in previous studies [8-10]. Unfortunately, the greatest uncertainty to face was the calibration sources themselves. Nevertheless, as the main goal here was to evaluate the ability to differentiate between samples, the calibration precision was not a critical point, as the main thing to demonstrate was the existence of relative differences.

Coincidence corrections

A very important matter to deal with, while using high efficiency HPGe detectors, is the coincidence correction for each nuclide activity. In the case of a nuclide decaying through a cascade of successive photon emissions measured with a high efficiency detector, both coincidence losses and coincidence summing effects in the peak, are important.

The GESPECOR allows evaluation of the coincidence-summing effects for any peak which might be present in the spectrum, from all frequently encountered nuclides. From the computational point of view, it is useful to consider separately three types of peaks:

– the first type is represented by the *normal* peaks, *i. e*. peaks associated with individual photons emitted in the decay process of the nuclide. This is the common type of peaks, present in the spectra both in the case when coincidence-summing effects are absent and when they are present,
– the second type is represented by pure gamma-ray sum peaks, and
– the third type of peaks is represented by sum peaks in which at least one contribution occurs to summing results from X-ray photon absorption. Such peaks are observed in the spectra only if the detec-

* map source: DOI 10.1007/s13762-024-06128-z
**Credits: Dr. M. Iovea

tor efficiency at low energies (in the region of X-rays) is high.

The coincidence correction factor (Fc) in GESPECOR is defined as the ratio of the apparent efficiency for the energy E of the nuclide with coincidence-summing effects, to the efficiency for the same energy obtained from the efficiency calibration curve measured with nuclides with negligible coincidence-summing effects. The apparent efficiency for a normal peak of the nuclide in question is defined as the count rate in the full energy peak divided by the product of the nuclide activity with the yield of the corresponding gamma ray; in the case of a pure sum peak, the apparent efficiency is defined as the count rate in the full energy peak divided by the nuclide activity. The Fc is a measure of the coincidence-summing effects. For regular peaks it is equal to 1 if the effects are absent, smaller than 1 if the coincidence losses from the peak are prevailing, and greater than 1 if coincidence summing up in the peak is the dominating factor. In tab. 2 below, Fc stands for coincidence correction factor, Nsec and Nsum represent the number of different secondary photons that may be emitted in transitions belonging to cascades including the transition of interest (Nsec), respectively the number of different combinations of transitions contributing as sum peaks to the peak of interest (Nsum). Ideal Ef stands for ideal efficiency and Err (%) is the statistical uncertainty.

Measurements and calculations

The acquisition time for the spectra is typically 24 h, in order to have good statistics in the peaks. Dead time calculation was performed by the default Gadke-Hale algorithm from ORTEC Maestro32 [11]. Blank boxes were also analyzed just as the sample, in order to correctly extract the background and improve accuracy.

For this batch of samples, the 46 keV line of ^{210}Pb for dating purposes was tested on a *n*-type detector for one sample from each region; the results were systematically above the detection limit within a few hours. Nevertheless, this was just a confirmation of feasibility, as such measurements have been performed in the area, although not in a systematic manner [12]. The entrance window of the main detector was Al 0.5 mm thick, instead of the required Be of about 50 microns. Consequently, in the view of an enlarged study the p type detector needs to be replaced by a *n*-type one, so this procedure will allow dating by ^{210}Pb measurements additionally to measurements on natural series, isotopic patterns and artificial contamination testing. The overall related uncertainty was estimated to some 11 %, mainly due to the fact that the calibration source was an old one with poor statistics and it exhibits a non-homogenous matrix contraction within the container. Regarding the lithology, the description related to the samples studied is given in tab. 3.

RESULTS AND DISCUSSION

For the batch of samples described, the results are presented in tab. 4 from the results section. In order to have a clear picture of the differences between the samples, the results are normed to the highest activity recorded per radionuclide from the batch (no matter which particular sample the result originates from). For the 186 keV peak, which is obviously a convolution of ^{235}U and ^{226}Ra, given the half-lives and yields for the components, the fraction to be accounted for the ^{235}U contribution is 43 %; the rest belongs to ^{226}Ra. The emission yields are 57.2 % for the 185.7 keV line of ^{235}U ($T_{1/2}$ = 7.04·108 year) and 3.64 % for the 186.2 keV line of ^{226}Ra ($T_{1/2}$ = 4.47·109 year for ^{238}U). This is valid only while admitting equilibrium in the natural series. The 43 % ratio derives from the equation

Table 2. Coincidence correction factors for some nuclides involved in the analysis

Nuclide	Decay	Energy [keV]	Yield	Fc	Nsec	Nsum	Ideal Ef	Err [%]
^{137}Cs	Beta	661.66	$0.8499\cdot10^{0}$	$0.10000\cdot10^{1}$	0	0	0.29106-01	0.11 + 00
^{40}K	EC	1460.82	$0.1066\cdot10^{0}$	$0.10000\cdot10^{1}$	1	0	0.16681-01	0.24 + 00
^{210}Pb	Beta	46.54	$0.4252\cdot10^{-1}$	$0.10000\cdot10^{1}$	0	0	0.14314-01	0.94-01
^{214}Pb	Beta	242.00	$0.7268\cdot10^{-1}$	$0.99607\cdot10^{0}$	2	0	0.61636-01	0.71-01
^{214}Pb	Beta	295.22	$0.1841\cdot10^{0}$	$0.10010\cdot10^{1}$	1	1	0.53367-01	0.47-01
^{214}Pb	Beta	351.93	$0.3560\cdot10^{0}$	$0.99870\cdot10^{0}$	1	0	0.46486-01	0.92-01
^{214}Bi	Beta	609.31	$0.4549\cdot10^{0}$	$0.87989\cdot10^{0}$	57	0	0.30891-01	0.13 + 00
^{214}Bi	Beta	768.36	$0.4891\cdot10^{-1}$	$0.85092\cdot10^{0}$	21	0	0.26194-01	0.15 + 00
^{214}Bi	Beta	934.06	$0.3099\cdot10^{-1}$	$0.85952\cdot10^{0}$	11	2	0.22904-01	0.13 + 00
^{214}Bi	Beta	1120.29	$0.1491\cdot10^{0}$	$0.86586\cdot10^{0}$	6	1	0.20133-01	0.18 + 00
^{214}Bi	Beta	1238.11	$0.5830\cdot10^{-1}$	$0.87167\cdot10^{0}$	4	3	0.18794-01	0.13 + 00
^{214}Bi	Beta	1377.67	$0.3967\cdot10^{-1}$	$0.10471\cdot10^{1}$	20	1	0.17373-01	0.14 + 00
^{214}Bi	Beta	1729.59	$0.2843\cdot10^{-1}$	$0.12634\cdot10^{1}$	5	2	0.14600-01	0.17 + 00
^{214}Bi	Beta	1764.49	$0.1531\cdot10^{0}$	$0.10026\cdot10^{1}$	4	5	0.14387-01	0.21 + 00
^{214}Bi	Beta	2204.21	$0.4912\cdot10^{-1}$	$0.10036\cdot10^{1}$	2	10	0.11978-01	0.19 + 00
^{226}Ra	Alpha	186.21	$0.3555\cdot10^{1}$	$0.10000\cdot10^{1}$	0	0	0.72705-01	0.92-01
^{235}U	Alpha	143.77	$0.1094\cdot10^{0}$	$0.99843\cdot10^{0}$	5	0	0.80345-01	0.71-01
^{235}U	Alpha	185.72	$0.5700\cdot10^{0}$	$0.99055\cdot10^{0}$	4	0	0.72692-01	0.12+00

Table 3. Sediment sample lithological description.

Code/number	Lithology and other textural observations	Environment
DD-19-01/SPL1*	Fine – medium sand, rich in shells	Fluvial (natural)
DD-19-08/SPL2	Medium sand, frequent pebbles, rich in organic matter	Fluvial (natural)
DD-19-11/SPL3	Compact clay	Fluvial (natural)
DD-19-16/SPL4	Fine sand with millimeter-sized muddy elements	Fluvial (natural)
DD-19-17/SPL5	Compact silty clay	Fluvial (natural)
DD-19-20/SPL6	Fine/medium sand	Fluvial (natural)
DD-19-23/SPL7	Fine/medium sand, frequent pebbles and anthropic elements	Fluvial (natural)
DD-19-26/SPL8	Silty clay covered by 2 cm of fine sand, frequent pebbles	Fluvial (natural)
DD-19-29/SPL9	Compact clay covered by fine gravel	Fluvial (natural)
DD-19-32/SPL10	Sandy mud with frequent pebble, rich in shells	Fluvial (natural)
DD-19-33/SPL11	Fine/medium sand with numerous shells	Fluvial (natural)
DD-19-36/SPL12	Fine mud	Fluvial
DD-19-38/SPL13	Silty mud covered by 2 cm of fine – medium sand	Fluvial (natural)
DD-19-41/SPL14	Fine mud with pebbles	Fluvial (natural)
DD-19-44/SPL15	Fine sandy mud	Fluvial
DD-19-45/SPL16	Fine/medium sand with numerous shells, muddy elements	Fluvial (natural)
DD-19-48/SPL17	Fine/medium sand with frequent shells	Fluvial
DD-19-49/SPL18	Fine/medium sand with frequent shells	Fluvial (natural)
DD-19-117/SPL19	Fine mud rich in organic matter	Lacustrine

Table 4. Specific activities normed to the highest value from the first Lower Danube lot, Danube Delta area. Blank sample areas were subtracted from the activity values

[dless]**	^{235}U	^{226}Ra	^{212}Pb	^{214}Pb	^{208}Tl	^{214}B	^{137}Cs	^{228}Ac	^{40}K
SPL1	0.8188	0.8188	0.7165	0.7403	0.7508	0.8235	0.0128	0.7795	0.7396
SPL2	0.5084	0.5084	0.4605	0.4459	0.4679	0.4960	0.0000	0.4957	0.4471
SPL3	1.0000	1.0000	0.8170	0.7343	0.8574	0.7996	0.2471	0.8234	0.7774
SPL4	0.3648	0.3649	0.3813	0.4146	0.4381	0.4862	0.0639	0.4812	0.4934
SPL5	0.6196	0.6196	0.7652	0.7047	0.7811	0.7675	0.0000	0.7230	0.7212
SPL6	0.4398	0.4398	0.3783	0.3959	0.4220	0.4661	0.0395	0.4257	0.5032
SPL7	0.6315	0.6315	0.6010	0.5897	0.6816	0.6297	0.0739	0.6036	0.5476
SPL8	0.8325	0.8325	0.7402	0.8158	0.7587	0.8684	0.0412	0.6931	0.7121
SPL9	0.9547	0.9547	0.9296	0.9660	0.9103	0.9401	0.0982	0.8068	0.4810
SPL10	0.5652	0.5652	0.7478	0.7664	0.7433	0.8139	0.0124	0.7064	0.7187
SPL11	0.8316	0.8317	0.8836	0.9261	0.8858	0.9554	0.0000	0.8174	0.6800
SPL12	0.6214	0.6214	0.4327	0.5033	0.5156	0.5985	0.0086	0.4764	0.5605
SPL13	0.3093	0.3093	0.4130	0.4289	0.4007	0.5341	0.0181	0.4694	0.4386
SPL14	0.3665	0.3665	0.2446	0.4714	0.4015	0.5061	0.0000	0.4021	0.4921
SPL15	0.3560	0.3603	0.3001	0.6012	0.4904	0.6387	0.0336	0.5194	0.6183
SPL16	0.7128	0.9690	0.6475	1.0000	0.8185	0.9617	0.0000	0.7932	0.6510
SPL17	0.5905	0.5905	0.6217	0.9214	0.7622	0.9575	0.0916	0.6730	0.6577
SPL18	0.8456	0.8456	0.7000	0.9355	0.8521	0.9354	0.1377	0.7865	0.6569
SPL19	0.5450	0.5450	0.6018	0.7864	0.7396	0.7932	0.0072	0.6481	0.7104

$$\frac{R(^{235}\mathrm{U})}{R(^{226}\mathrm{Ra})}=\frac{A(^{235}\mathrm{U})\cdot s_{186}(^{235}\mathrm{U})}{A(^{226}\mathrm{Ra})\cdot s_{186}(^{226}\mathrm{Ra})}=$$
$$=\frac{\frac{\ln 2}{T_{1/2}(^{235}\mathrm{U})}\cdot N(^{235}\mathrm{U})\cdot s_{186}(^{235}\mathrm{U})}{\frac{\ln 2}{T_{1/2}(^{236}\mathrm{Ra})}\cdot N(^{226}\mathrm{Ra})\cdot s_{186}(^{226}\mathrm{Ra})}=$$
$$=\frac{4.47\cdot 10^{9}\,a}{7.04\cdot 10^{8}\,a}\cdot 0.0072\cdot\frac{57.2}{3.53}=0.74$$

where *R* stands for nuclide count rate in counts per second, A for nuclide activity in disintegrations per second, *s* for scheme factor or yield, $T_{1/2}$ for half-life in years (a being from the Latin *annum*) and *N* for number of counts. Consequently, the counting rate at equilibrium for ^{235}U is 0.74 times the counting rate for ^{226}Ra in their common peak at 186 keV, so the fraction of the count rate for ^{235}U is $f_{186}(^{235}\mathrm{U}) = 0.74 / (1 + 0.74) = 43$ %.

This leads to the specific activities in Bqkg^{-1}, which are presented in tab. 4, as normed (dimensionless) to the highest value found in the batch, in order to provide a better picture of the range.

By way of example, as the results were presented as normed to the highest value, here are some maximum absolute values for the batch: 1 Bqkg^{-1} for ^{137}Cs, 38 Bqkg^{-1} for ^{212}Pb, 34 Bqkg^{-1} for ^{214}Pb, Bqkg^{-1} for ^{40}K,

*"SPL" stands for sample, "dless" for dimensionless quantity

which are within the normal limits. But the scope is to get a visual approach on the relative differences between samples from different areas and also originating from the same area, as pictured in fig. 3.

Also, this provides a visual approach on the relative differences between samples from different areas and also originating from the same area, as shown in fig. 3.

In fig. 3, according to the map from fig. 1, positions 1 and 2 represent the tests for the Chilia Veche branch; positions 3 to 10 and 19 belong to the first sampling area; positions 11 to 18 represent the second area. Note: smooth lines represent the contributions from natural series, the staked line belongs to ^{40}K (non-series), and the (low) green line shows ^{137}Cs variations within the batch.

One can easily observe the variations within and between the sampling areas are as high as 50 %, with a mean of some 25 % between the spots; additionally, the smooth lines related to the natural series have a common pattern evolution, which brings confidence in data consistency. The ^{40}K variations are also important, showing each spot does have its own characteristics. ^{137}Cs activity has significant variations for an isotopic pattern, although within the normal range for the concerned area, as the latter is only 690 km south from Chernobyl.

Considering the location of the sediments, as well as their composition in terms of granulometry and other present elements (*i. e*., shells, pebbles, organic matter, *etc*.), several correlations can be pointed out. With reservation into interpreting these correlations for a small batch, compact clay samples seem to exhibit a typical pattern richer in natural series elements, as well as the sandy material. In contrast with the abovementioned clay and sand, muddy samples display lower activities for those decay chains. Besides contamination factors, the lithological and textural composition that usually respects the environment and location characteristics is connected to the variations seen in the spectrometric reports.

Covariance matrices are clearly the way to be followed for the database to be started, as additionally neutron activation of the samples evidenced markers such as ^{24}Na, ^{42}K, ^{183}Ir, ^{56}Mn, ^{24}Al, ^{57}Ni, ^{36}P, ^{183}Hg in different quantities for this batch of samples. Thus, given the fact the Pu-Be source used was not yet characterized properly, it can only be reported the possibility of tracking such radioelements for the moment. The aim is to repeat the study from reference [13] and to obtain more information from the regulatory commission on such sources made back in the 50's in the former Soviet Union in order to obtain quantitative determinations. Recent examples of such studies in this field are given in the papers of Olacel *et al*. [14] and Bui *et al*. [15]. Another goal is to develop the study towards transfer factor analysis, such as in [16].

CONCLUSIONS

Several samples from the Lower Danube area were analyzed by means of gamma spectrometry in order to see if this study can be a good forerunner for generating a Danube Reference Material Database.

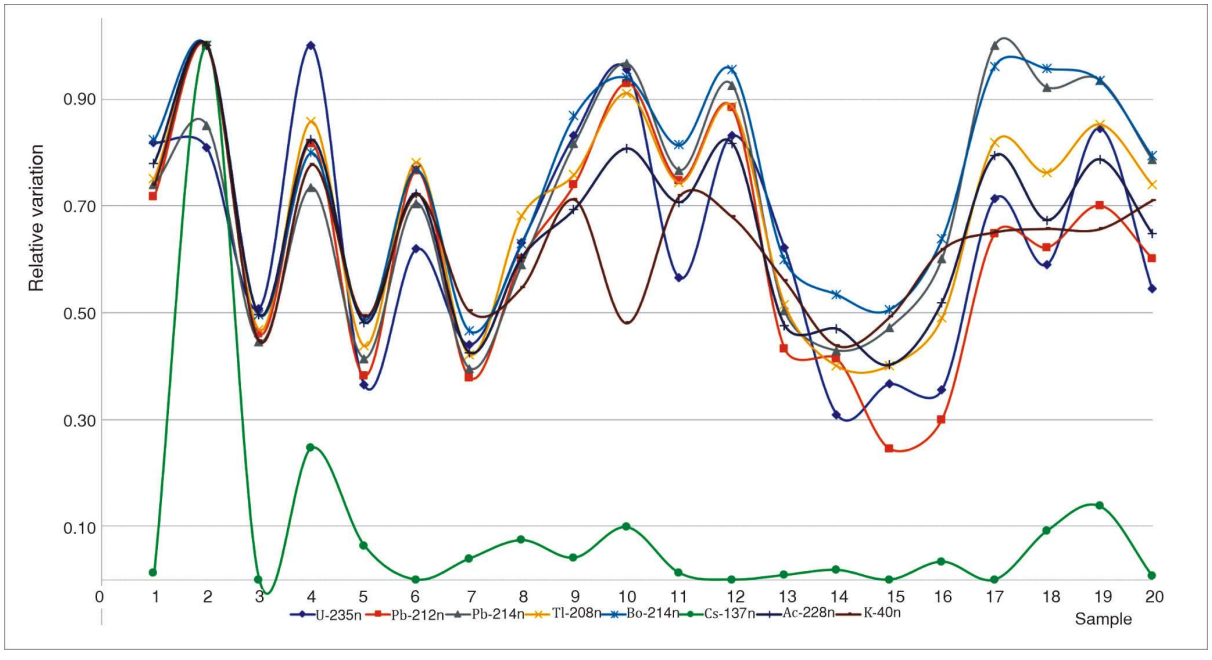

Figure 3. Relative variations of selected TENORM nuclides from the batch, indexed with respect to the locations

For ensuring good quality data, there is a need to gather information on the recent history of the sampling area concomitantly, as it may involve anthropogenic influence, such as small interferences with civil works performed in the area and upstream, or other contamination mechanisms. The results support the hypothesis in the sense that: samples from a certain area can be considered overall characteristic and samples from a small area exhibit differences that would allow tracking modifications in the future, if such will be the case.

This means the samples analyzed provided valuable information which motivates further developments and adapting the laboratory equipment in order to continue the analysis process on a larger scale, adding the dating procedure with ^{210}Pb and investigating other anthropogenic contributions to the spectra (Am, Co, Pu, *etc*.).

Nevertheless, it is mandatory to refine the method in terms of detector window and Germanium dead layer thickness (using only Beryllium or Carbon front entrance window *n*-type detectors), to increase shielding thickness and sample mass, and test sample uniformity, as the latter is accountable for notable contributions in the uncertainty budget. This would allow the use of covariance matrices in order to take tracking and concentration dynamics to the next level. Also, the plan is to further use X-ray analysis and neutron activation for getting complementary information on the isotopic patterns (as following neutron irradiation stable elements turn into beta emitters, which subsequently provide characteristic gamma rays), which strengthen the pattern identification procedure. Neutron activation proved feasible, but not quantitatively yet.

AUTHORS' CONTRIBUTIONS

I. Pojar Vintila – conceptualization, investigation, writing – review and editing; S. Ujeniuc – data curation, methodology, software, supervision, validation; I. Catianis – conceptualization, investigation; B. Alexandrescu – formal analysis, methodology, resources; A. M. Scrieciu – conceptualization, investigation; S. Vasilca - data curation, software; R. Suvaila - conceptualization, formal analysis, methodology, validation, writing original draft, review and editing.

ORCID ID

I. Pojar Vintila: 0000-0002-5209-4489
S. Ujeniuc: 0009-0002-9669-7414
I. Catianis: 0000-0001-8120-7369
S. Vasilca: 0000-0001-9149-9481
R. Suvaila: 0000-0001-6463-8685

REFERENCES

[1] Deniz, K., Calik, A. E., Hazard Assessment of Outdoor Gamma Radiation in Tavsanli, Kutahya Region of Turkiye, *Nucl Technol Radiat, 39* (2024), 1, pp. 74-80
[2] Janković, M., *et al*., Natural or Artificial Tritium in Rivers – the Assessment Using Symmetrical Index, *Nuclear Engineering and Design, 427* (2024), 113419
[3] Pojar, I., *et al*., Sedimentary Microplastic Concentrations from the Romanian Danube River to the Black Sea, *Scientific Reports, 11* (2021), Jan., 2000
[4] ***, IAEA TECDOC 1783 International Atomic Energy Agency Vienna (2016), March
[5] Sima, O., Arnold, D., Dovlete, C., GESPECOR: A Versatile Tool in Gamma-Ray Spectrometry, *Journal of Radioanalytical and Nuclear Chemistry, 248* (2001), May, pp. 359-364
[6] Sima, O., Arnold, D., Transfer of the Efficiency Calibration of Germanium Gamma-Ray Detectors Using the GESPECOR Software, *Applied Radiation and Isotopes, 56* (2002), 1-2, pp. 71-75
[7] Suvaila, R., *et al.*, Gamma Ray Spectroscopy for Artificial Contamination Effects Evaluation in Luminiscence Dating of Artefacts from Low Depth Layers in Southern Romania, *Romanian Reports in Physics* (2012), 2, pp. 381-386
[8] Suvaila, R., Stancu, E., Sima, O., On Within Sample Homogeneity Testing Using Gamma-Ray Spectrometry, *Applied Radiation and Isotopes, 70* (2012), 9, pp. 2144-2148
[9] Suvaila, R., Osvath, I., Sima, O., Improving the Assessment of Activity in Samples with Non-Uniform Distribution Using the Sum Peak Count Rate, *Applied Radiation and Isotopes, 81* (2013), Nov., pp. 76-80
[10] Suvaila, R., Sima, O., Osvath, I., Improved Method for the Assessment of ^{60}Co and ^{134}Cs Point Sources in Samples with Non-Homogeneous Matrix, *Applied Radiation and Isotopes, 87* (2014), May, pp. 384-386
[11] ***, www.orterc-online.com ORTEC PN. 777800 0812 Manual Revision, P, 2012
[12] Dovlete, C., *et al*., Gamma Spectrometric Measurement of ^{210}Pb in Environmental Samples, *Environment International, 22* (1996), Supplement 1, pp. 319-321
[13] Söderström, P.-A., *et al.*, Characterization of a Plutonium-Beryllium Neutron Source, *Applied Radiation and Isotopes, 167* (2021), 109441
[14] Olacel, A., *et al*., Isotopic Patterns Via Neutron Irradiation and Gamma Spectrometry of Environmental Samples, *Chemical Physics Impact, 4* (2022), 100065
[15] Bui, T.-H., *et al*., Characteristics of Natural Radionuclides and ^{137}Cs in Surface Soil in Phonsavan, Xiengkhouang, Laos, *Nucl Technol Radiat, 38* (2023), 4, pp. 289-300
[16] Vukašinović, I. Ž., Analysis of ^{238}U, ^{226}Ra, and ^{210}Pb Tranfer Factors from Soil to the Leaves of Broadleaf Tree Species, *Nucl Technol Radiat, 37* (2022), 3, pp. 219-228

Received on August 5, 2024
Accepted on December 10, 2024

Јулијан ПОЖАР ВИНТИЛА, Сорин УЖЕНИЈУК, Ирина КАЦИЈАНИС, Богдан АЛЕКСАНДРЕСКУ, Албер М. СКРИЈЕЧУ, Силвана ВАСИЛИКА, Рареш ШУВАЈЛА

ГАМА СПЕКТРОМЕТРИЈСКА АНАЛИЗА УЗОРАКА ДОЊЕГ ДУНАВА, РУМУНИЈА

Рад се фокусира на природну и антропогену радиоактивност узорака седимената са кључних места лоцираних у области Доњег Дунава и региону делте Дунава. Намера је да се потврди да је гама спектрометрија ефикасан метод за карактеризацију геолошких узорака у смислу изотопских односа, као и за процену утицаја нуклеарних активности, односно тестирање вештачке контаминације. Ово је прелиминарна студија која има за циљ да анализира релевантност базе података за референтне седименте из реке Дунав, изграђене путем спектрометрије гама зрачења.

Кључне речи: геолошки узорак, изотопска заступљеност, екологија, гама спектар